Comparison of Dye-Sensitized Rutile- and Anatase-Based TiO_2 Solar Cells

N.-G. Park,* J. van de Lagemaat, and A. J. Frank*

National Renewable Energy Laboratory, Golden, Colorado 80401

Received: December 10, 1999; In Final Form: June 8, 2000

Crack-free nanocrystalline rutile TiO_2 films with thicknesses of up to 12 μm were prepared and characterized in connection with their application to dye-sensitized solar cells. The photoelectrochemical properties of the rutile-based solar cell are compared with those of the anatase-based cell. Scanning electron microscopy (SEM) shows that the rutile films consist of homogeneously distributed rod-shaped particles with an average dimension of 20 × 80 nm. Both the thickness and the morphology of the rutile films have a strong influence on the photoelectrochemical properties of the solar cells. Measurements of the incident monochromatic photon-to-current conversion efficiency (IPCE) as a function of film thickness imply that a significant fraction of light in the spectral region below 600 nm is absorbed in the first few microns of the dye-covered films due to strong light absorption by the dye. At longer wavelengths, where the dye absorbs weakly, the IPCE increases in direct proportion to the film thickness, suggesting that the electron-injection rate throughout the cell approaches homogeneity. The open-circuit photovoltage (V_{oc}) shows only a small change with film thickness, which is attributed to the compensating effect associated with the dependence of the number of dye molecules and recombination centers on the surface area. For the same film thickness, the photocurrent−voltage responses of the dye-sensitized rutile and anatase films at one-sun light intensity are remarkably close. Their V_{oc} is essentially the same, whereas the short-circuit photocurrent of the rutile-based cell is only about 30% lower than that of the anatase-based cell. The lower photocurrent of the rutile film correlates with a lesser amount of adsorbed dye, owing to a smaller surface area per unit volume compared with that of the anatase film. Intensity-modulated photocurrent spectroscopy and SEM studies indicate that electron transport is slower in the rutile layer than in the anatase layer due to differences in the extent of interparticle connectivity associated with the particle packing density.

Introduction

Interest in the study of dye-sensitized nanocrystalline metal oxide solar cells has grown considerably in recent years from both a fundamental and an applied perspective. The metal oxide is the recipient of injected electrons from optically excited dye molecules and provides the conductive pathway from the site of electron injection to the transparent back contact.[1] The redox species in solution transports the hole from the oxidized dye to the counter electrode, thus completing the redox cycle. The metal oxide can strongly influence the photovoltage, the fill factor, and the photon-to-current conversion efficiency (IPCE), which is determined by the light-harvesting efficiency of the dye, the quantum yield of electron injection, and the efficiency of collecting the injected electrons. Although a few studies have explored semiconducting oxides such as SnO_2,[2] ZnO,[3] Nb_2O_5,[4] CeO_2,[5] and $SrTiO_3$,[6] the preponderance of work has focused on the anatase form of TiO_2.[7] Little attention has been paid to the rutile form of TiO_2. Rutile TiO_2 is the most commonly used white pigment in paints. It is favored over anatase for this purpose because the rutile scatters white light more efficiently and is chemically more stable.[8] For photocatalysis, however, anatase is perceived as the more active phase of TiO_2 because of its surface chemistry and potentially higher conduction-band edge energy.[9] Perhaps because of the latter property, anatase has been the choice material for dye-sensitized solar cells, even though rutile is potentially cheaper to produce and has superior light-scattering characteristics, which is a beneficial property from the perspective of effective light harvesting.

Recently, we showed that dye-sensitized solar cells based on rutile TiO_2 exhibit photovoltaic characteristics at one-sun light intensity comparable to those of conventional anatase TiO_2-based solar cells.[10] Nanocrystalline rutile films were directly deposited onto the transparent back contact from the ambient hydrolysis of $TiCl_4$ and subsequently annealed. High quality films prepared by this method were limited to thicknesses of less than 5 microns. This is well below the requisite thickness for achieving, from an applied perspective, an adequate electron injection current from a monolayer of a Ru-bipridyl based charge-transfer dye adsorbed onto the TiO_2 surface.

In this paper, we describe a new method for preparing crack-free, nanocrystalline rutile TiO_2 films of up to 12 μm in thickness. The effect of film thickness and morphology on the photoelectrochemical properties is examined. The photovoltaic characteristics of rutile-based solar cells are compared with those of anatase-based solar cells. Information on electron transport in the nanoporous rutile films is obtained by intensity-modulated photocurrent spectroscopy IMPS.

Experimental Section

Nanocrystalline rutile TiO_2 particles were formed as a precipitate from the hydrolysis of $TiCl_4$ (Aldrich) as follows: $TiCl_4$ was added dropwise to chilled water (~ 4 °C) to obtain a concentration of 2 M TiO_2. Subsequently, the solution was diluted to 0.5 M TiO_2 and set aside in a closed, air-filled vessel for 5 days. The liquid was then removed with a rotary evaporator. The resulting white precipitate was repeatedly

10.1021/jp994365l CCC: $19.00
Published on Web 09/01/2000

purified by the addition of distilled water followed by its removal by rotary evaporation. These steps were then repeated using methanol in place of water. The dried precipitate was collected and redispersed in distilled water to produce a solution containing 15 wt % TiO_2. With respect to the amount of TiO_2 present, to the TiO_2 colloid solution were added 20 wt % poly ethylene glycol (Aldrich, average MW 2000) and 15 wt % poly ethylene oxide (Polysciences, average MW 100 000), which was then stirred for 2 days with a magnetic stirring bar, to yield the slurry. The resulting slurry was spread with a doctor blade onto a transparent electrical conducting SnO_2 coated glass substrate (Libbey-Owens-Ford Co., TEC-10 (10 ohm/sq), 75% transmittance in the visible), dried at 100 °C for 10 min and subsequently heated in air for 1 h at 500 °C.

X-ray diffraction and Raman spectroscopy measurements[10] confirmed the phase purity of the annealed TiO_2 films as rutile; no impurities were evident. The thickness of the transparent rutile films was measured with a Tencor Alpha-step profiler. Up to 12 μm thick crack-free rutile films could be fabricated by this procedure. The morphology of the TiO_2 films was investigated by field emission scanning electron microscopy (SEM; JEOL Model 6320F). The preparation of transparent nanocrystalline anatase TiO_2 films is described elsewhere.[11]

For photosensitization studies, the TiO_2 electrodes were immersed in acetonitrile/*tert*-butyl alcohol (50:50 v/v%) containing 3×10^{-4} M Ru(LL′)$(NCS)_2$ (where L = 2,2′-bipyridyl-4,4′-dicarboxylic acid, and L′ = 2,2′-bipyridyl-4,4′-ditetrabutylammoniumcarboxylate) for 24 h at room temperature. The dye-covered electrodes were then rinsed with the acetonitrile/*tert*-butyl alcohol mixture and dried under a N_2 stream. To minimize re-hydration of TiO_2 from moisture in the ambient air, the electrodes were immersed in the dye solution while they were still warm (100−120 °C) from the annealing step. Pt counter electrodes with a mirror finish were prepared by electron beam deposition of a 60 nm layer of Pt on top of a 40 nm layer of Ti on a glass plate. The Pt electrode was placed over the dye-coated TiO_2 electrode and the edges of the cell were sealed with 0.5-mm wide stripes of 25-μm thick Surlyn (Dupont, grade 1702). Sealing was accomplished by pressing the two electrodes together at a pressure of 900 psi and a temperature of about 120 °C. The redox electrolyte, consisting of 0.6 M 1,2-dimethyl-3-hexyl imidazolium iodide, 0.2 M LiI, 40 mM I_2, and 0.2 M *tert*-butyl pyridine in acetonitrile, was introduced into the cell through one of two small holes drilled in the counter electrode. The holes were then covered and sealed with small squares of Surlyn 1702 and microscope objective glass. The resulting cell had an active area of about 0.3 cm^2.

Photocurrent−voltage $J-V$ measurements were performed using a Keithley Model 236 source measure unit. A 1000-W sulfur lamp (Fusion Lighting Inc.) served as a light source, and its light intensity (or radiant power) was adjusted with a Si solar cell equipped with KG-5 filter (Schott) for approximating AM-1.5 radiation. The light source for the incident photon-to-current conversion efficiency IPCE measurements was a 150-W Quartz halogen lamp equipped with a Photon Technology International Model 1492 monochromator. The intensity was measured with a UDT Instrument Model S370 optometer and a UDT Instrument Model 221 calibrated photodiode. UV−vis absorption spectra of the dye-covered rutile and anatase films on the conducting glass substrates were measured with a HP 8450A diode-array spectrophotometer. The spectra of the dye-covered films were referenced to those of the respective dye-free samples of the rutile and anatase films. To further minimize light-scattering effects, the samples were positioned as close to detector as possible, and the probe beam from the spectrophotometer entered the conducting glass substrate before passing through the films to the detector. The setup for the intensity-modulated photocurrent spectroscopy (IMPS) measurements is described elsewhere.[12] In the IMPS studies, the samples were illuminated with 680-nm wavelength light, which is only weakly absorbed by the dye.

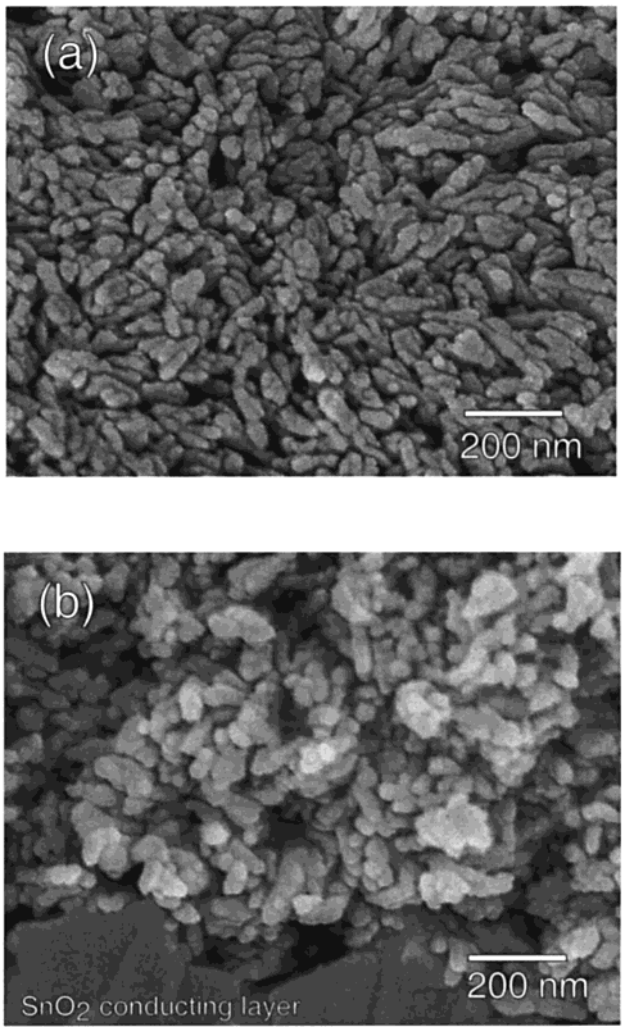

Figure 1. Scanning electron microscope micrographs showing the (a) surface and (b) cross section of an 11.5-μm thick rutile TiO_2 film that was deposited on conducting glass from a colloidal slurry and subsequently annealed at 500 °C for 1 h.

Results and Discussion

Rutile. Figure 1 shows surface and cross-section SEM micrographs of an annealed rutile film. The film is composed of rod-shaped particles with an average dimension of 20 × 80 nm. It can be seen that the particles show no preferred orientation and are distributed homogeneously throughout the film. Furthermore, the particle density does not depend on film thickness (not shown).

Figure 2 shows the influence of film thickness on the $J-V$ characteristics of Ru(LL′)$(NCS)_2$-sensitized rutile TiO_2 solar cells at 1 sun light intensity. When the film thickness is increased from 5.0 ± 0.5 to 11.5 ± 0.5 μm, the short circuit photocurrent density J_{sc} increases by 62%, from 6.6 to 10.7 mA/cm^2. Concomitantly, the open-circuit voltage V_{oc} decreases from 759 to 727 mV. For a fixed density of particles in the film and homogeneously absorbed light (see discussion below), one

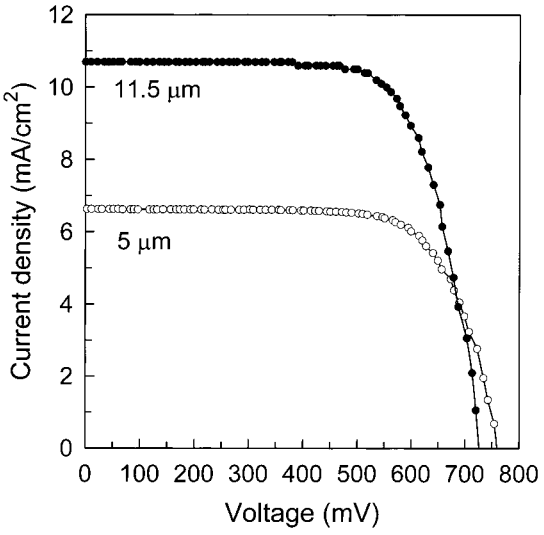

Figure 2. Effect of film thickness on the current−voltage characteristics of dye-sensitized rutile TiO_2-based solar cells at one-sun illumination.

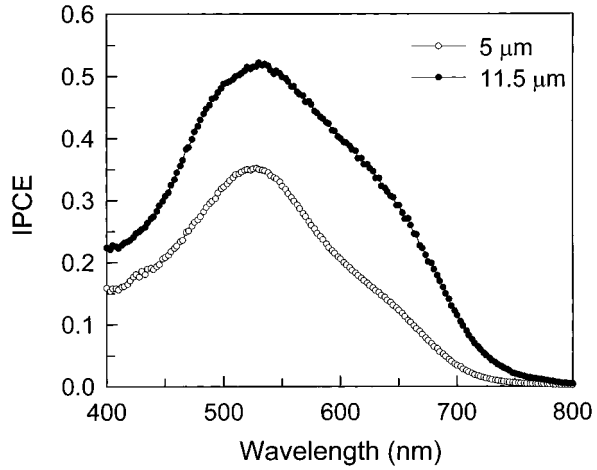

Figure 3. Effect of film thickness on the short-circuit IPCE values of dye-sensitized rutile TiO_2-based solar cells as a function of wavelength; no correction was made for reflection losses.

expects the electron injection-current density, and thus J_{sc}, to increase approximately linearly with film thickness, owing to the increased surface area of the film and therefore the increased number of adsorbed dye molecules. However, although the film thickness increases by 2.3-fold, J_{sc} only improves by 62%, implying that a significant fraction of the solar light is absorbed in the first 5 μm of the film. The small change (4%) in the open-circuit photovoltage with film thickness may be due to the offsetting effect connected with the dependence of the electron injection current and the number of recombination centers on surface area of the film. For example, as the film thickness is increased, the number of surface recombination centers is also expected to increase proportionately. Because the increased number of recombination sites (factor of 2.3) is somewhat larger than the increase of the electron injection-current density (factor of 1.6), a small decrease of V_{oc} is expected. The quantitative relation among the electron injection-current density, the number of recombination sites, and V_{oc} is discussed elsewhere.[13]

Figure 3 displays the incident monochromatic photon-to-current conversion efficiency (IPCE) of a 5 and 11.5-μm thick rutile film as a function of wavelength at short circuit. The IPCE is seen to increase considerably with film thickness. At the

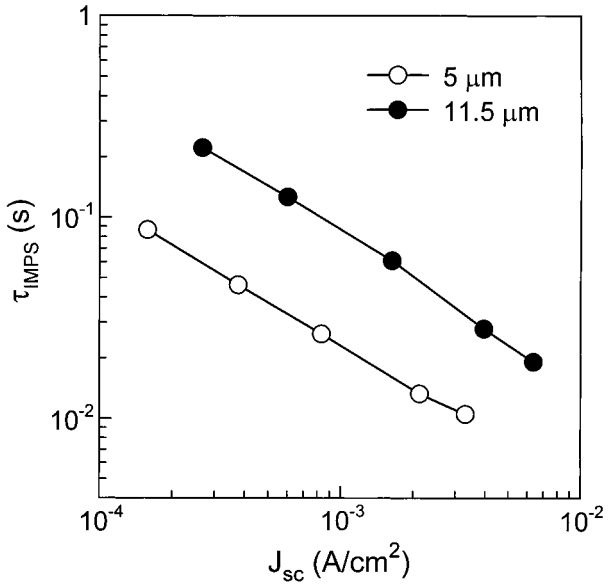

Figure 4. Effect of film thickness on the short-circuit IMPS time constant τ_{IMPS} as a function of the short-circuit current density J_{sc} at 680-nm illumination.

maximum value of the IPCE spectra at 530 nm, the IPCE of the 11.5-μm thick film is approximately 50% higher than that of the 5-μm thick rutile film. This increase is in good agreement with the increase of J_{sc} observed in Figure 2 when the cell is illuminated at (nonmonochromatic) one-sun light intensity. At a wavelength of 530 nm, the absorption of light by the dye-covered film is not homogeneous as one would expect based on the high extinction coefficient of the dye.[14] A significant fraction of the incident light is absorbed in the first 5-μm of TiO_2. At longer wavelengths (>600 nm), which the dye absorbs weakly, the increase of IPCE, relative to that of the 5-μm thick film, more closely matches the increase of film thickness, implying more uniform charge generation throughout the film. For example, at 680 nm the IPCE value increases by a factor of 2.9 when the film thickness increases by a factor of 2.3, essentially the same amount, within experimental error. This suggests that the electron-injection rate throughout the cell at this wavelength approaches homogeneity. It is also consistent with the charge-collection efficiency of the cell being unity at short circuit.[12]

Figure 4 shows the effect of film thickness on the short-circuit IMPS time constant τ_{IMPS} as a function of J_{sc} at 680-nm illumination. At short circuit, τ_{IMPS} gives the average time constant for the collection of photoinjected electrons at the back contact.[15] The IMPS time constants of both the 5 and the 11.5-μm thick samples decrease with increasing light intensity. This τ_{IMPS} dependence on light intensity (or J_{sc}) has been observed by ourselves and others[12,16−20] and has been attributed to an increase in the rate of electron transport resulting from the filling of deep (surface) traps by photoinjected electrons.[17,19−21] Figure 4 shows that at the same J_{sc}, τ_{IMPS} of the 11.5-μm thick sample is approximately 4.5 times larger than that of the 5-μm thick sample. Because electron transport occurs mainly by diffusion,[16−20,22] one expects from the relation $\tau_{IMPS} \propto d^2/D_n$ (where D_n is the effective diffusion constant of electrons in the film and d is the film thickness) that τ_{IMPS} should vary as d^2 for homogeneously absorbed light. This hypothesis is valid only in the absence of significant recombination at short circuit (i.e., when the charge-collection efficiency[12,15] is close to unity). This is likely the case here because the IPCE (Figure 3b) for 680-nm irradiation varies approximately linearly with film thickness.

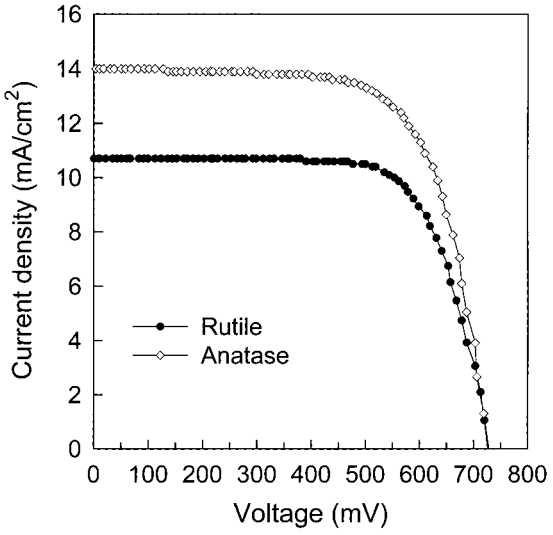

Figure 5. Comparison of the $J-V$ characteristics of dye-sensitized rutile- and anatase films of the same thickness (11.5 μm) at one-sun illumination.

If D_n is independent of film thickness at a given J_{sc}, then τ_{IMPS} is expected to increase by a factor of 5.3 ($\tau_{IMPS} \propto d^2/D_n$). Figure 4 shows that τ_{IMPS} increases by about a factor of 4.5, which is within experimental error of film-thickness and time-constant measurements.

Rutile and Anatase Comparison. Figure 5 shows that the $J-V$ characteristics of dye-sensitized rutile and anatase films of the same thickness (11.5 μm) at 1 sun light intensity are remarkably close. Their open-circuit voltages are about the same (730 mV), and J_{sc} of the rutile-based solar cell (10.6 mA/cm^2) is only about 30% less than that of the anatase-based cell (14 mA/cm^2). The respective overall energy conversion efficiencies of the rutile- and anatase-based cells are 5.6% and 7.1%. To understand the difference in their J_{sc}, we conducted SEM studies of their morphology.

Figure 6 shows top and cross sectional SEM micrographs of a rutile (Figures 6a and 6b) and an anatase (Figures 6c and 6d) film. The average dimensions of the rod-shaped rutile particles (20 $\times$ 80 nm; Figure 6a) are larger than that of the spherically shaped anatase particles (20-nm diameter; Figure 6c). Furthermore, it can be seen from a comparison of Figure 6b and 6d that the void volume (i.e., the total volume associated with the pores) of the rutile films appears larger than that of the anatase film, implying that the particle density, and thus the surface area per unit volume of the rutile film, is smaller than that of the anatase film. From the particle shape and size, it can be estimated that the surface area of the rutile film is at least 25% lower than that of the anatase film. This result suggests that the difference in the short-circuit photocurrent between rutile- and anatase-based cells (Figure 5) is due to their surface area (i.e., the amount of dye adsorbed). Support for this expectation is given below.

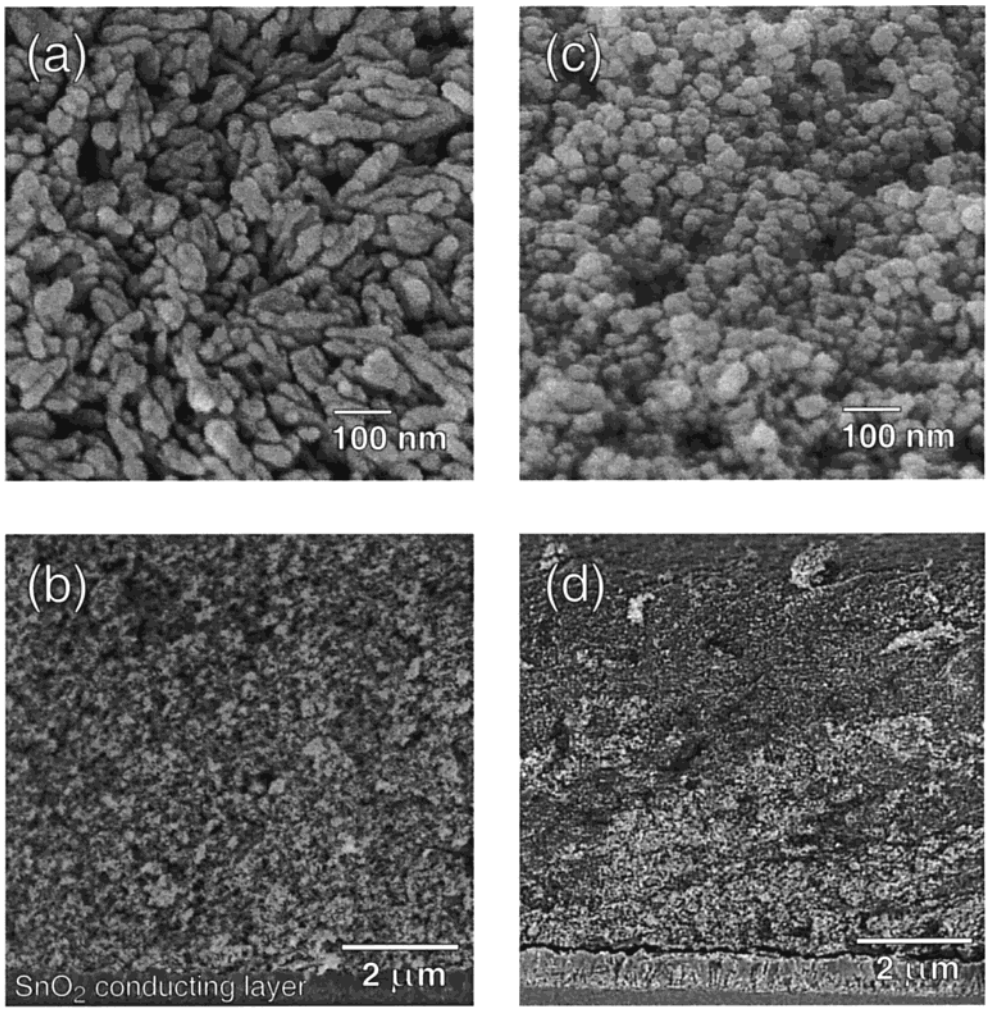

Figure 6. Surface and cross sectional SEM micrographs of a rutile (a, b) and an anatase (c, d) film coated on conducting glass and annealed at 500 °C for 1 h.

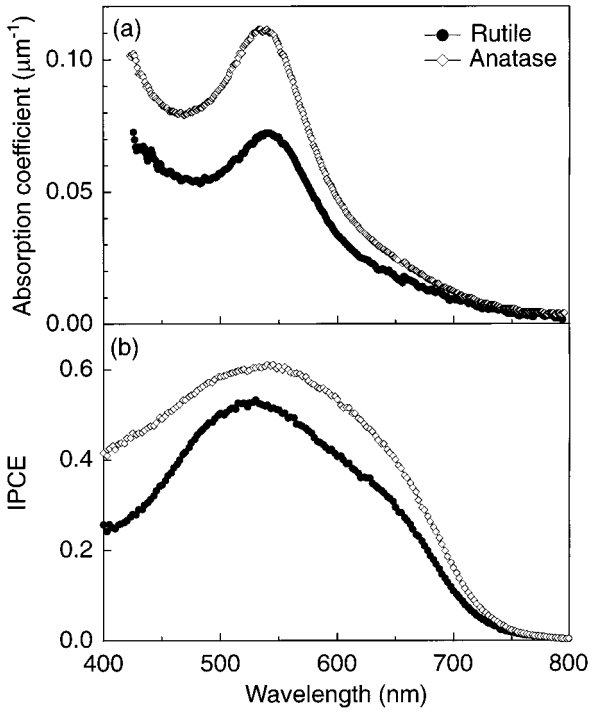

Figure 7. (a) Absorption spectra of dye-covered rutile and anatase films on the conducting glass substrates; spectra are referenced to those of the respective dye-free samples of the rutile and anatase films. (b) Short-circuit IPCE values of dye-sensitized rutile- and anatase films of the same thickness (11.5 μm) as a function of wavelength; no correction was made for reflection losses.

A comparison of the absorption spectra of the dye-covered rutile and anatase films indicates that the rutile film contains about 35% less adsorbed dye than the anatase film (Figure 7a). This number correlates with the estimated difference in surface area. The fraction of light absorbed by the dye is expected to determine their IPCE values. Figure 7b compares the short-circuit IPCE spectra of dye-sensitized rutile and anatase films of the same thickness (11.5 μm) at one-sun light intensity. Because the charge-collection efficiencies of the rutile (see discussion in connection with Figure 3) and anatase films[12] are essentially unity at short circuit and their quantum yields for electron injection are likely the same, the fraction of light absorbed by the dye is expected to determine their IPCE values. The IPCE of the rutile film at 530 nm is about 14% less than that of the anatase film, which is in accord with the difference in J_{sc} at one sun illumination (Figure 5). At long wavelengths (>550 nm), the difference in the ratio of their IPCE becomes larger, which is consistent with the rutile film containing a lower amount of adsorbed dye than the anatase film. In the short-wavelength spectral region (400−450 nm), the IPCE of the rutile film is about a factor of 2 lower than that of the anatase film. In this spectral region, iodide species (I_3^-) in the electrolyte absorb strongly, attenuating the amount of light reaching the sensitizing dye and thus limiting the photocurrent.[10] The relatively low IPCE value of the rutile film is thus a consequence of the presence of larger amounts of I_3^- in the pores of its more open structure (Figure 6b) compared with the compact structure of the anatase film (Figure 6d).

Figure 8 shows the effective electron diffusion coefficient D_n, measured by IMPS, as a function of J_{sc} at 680-nm illumination for dye-sensitized rutile and anatase films of the same thickness (11.5 μm). D_n is calculated from the relation $D_n = d^2/4\tau_{IMPS}$. This equation is valid only in the absence of recombination and for homogeneously absorbed light, which

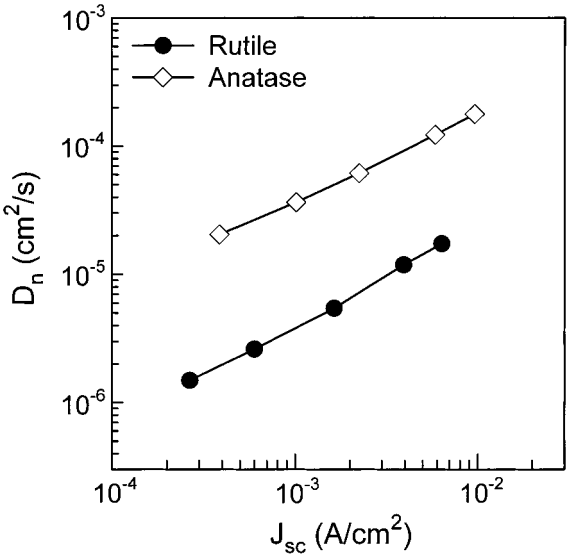

Figure 8. Comparison of the electron diffusion coefficient D_n of dye-sensitized rutile- and anatase films of the same thickness (11.5 μm) as a function of the short-circuit current density J_{sc} at 680-nm illumination.

is ensured by using 680-nm light as discussed in connection with Figure 4. As in the case of the dye-sensitized 11.5 μm thick rutile films, recombination is not important at short circuit for dye-sensitized anatase-based solar cells[12,15] for film thicknesses used in this study. The light intensity dependence of the electron diffusion coefficient for both rutile and anatase is attributed, as in the case of Figure 4, to the filling of deep (surface) traps by photoinjected electrons.[17,19−21]

In Figure 8, it can be seen that at the same J_{sc}, the effective electron diffusion coefficient D_n for the rutile film is about one order of magnitude lower than that of the anatase film, implying that electron transport is slower in the rutile layer than in the anatase layer. The difference in the rate of electron transport in these materials could be due to the number of surface states or the extent of interparticle connectivity per unit film volume. We first consider the possible role of surface states. It is generally accepted that the transport of electrons through the nanostructured film is slowed by multiple trapping events, involving principally surface states.[12,15,17,19−21] The number of surface states is generally proportional to the surface area of a film. If the number of surface states were the primary cause of the difference in the rate of electron transport in these materials, then one would expect that the surface area of the rutile film would be substantially larger than that of anatase. However, a comparison of the SEM micrographs in Figure 6b and 6d shows just the opposite, as discussed above. The surface area of the rutile film is smaller than that of the anatase film. On this basis, one would predict that electron transport would be faster in rutile than in anatase, which is contrary to the data in Figure 8. Thus, the absolute number of surface states can be ruled out as a cause for the *difference* in the rate of electron transport in rutile and anatase films. The second possible factor limiting electron transport involves the relative number of interparticle connections. In support of this possibility, a comparison of the morphology of the rutile (Figure 6a and 6b) and anatase (Figure 6c and 6d) films implies that within a given area or volume element, the number of nonspherically shaped, large sized (20 × 80 nm) rutile particles is less than that of the spherically shaped, small sized (20-nm diameter) anatase particles. These considerations lead to the conclusion that the rutile particles stack less efficiently than the anatase particles and that the rutile films have a lower number of interparticle connections per unit

film volume than that of the anatase film. Thus, the number of pathways encountered by an individual electron en route to the collecting electrode is effectively smaller for a rutile film than for an anatase film. Restricting the number of conductive pathways through the particle network is expected to slow electron transport through the rutile film and lower the electron diffusion coefficient.

Conclusions

Relatively thick, crack-free nanocrystalline rutile TiO_2 films were prepared from colloidal slurries. Contrary to the direct deposition method,[10] which limits the film thickness to several microns, films produced from the colloidal slurry have a thickness of up to 12 μm. The resulting rutile films consist of homogeneously distributed rod-shaped particles with average dimensions of 20 $\times$ 80 nm. IPCE measurements imply that a significant fraction of light with wavelengths below 600 nm is absorbed in the first few microns of the dye-covered films due to strong absorption by the dye. In the longer wavelength region, where the dye molecules absorb weakly, the short-circuit photocurrent increases in direct proportion to the film thickness, suggesting that the electron-injection rate throughout the cell approaches homogeneity. Contrary to the behavior of the short-circuit photocurrent, changing the film thickness has only a small influence on the open-circuit photovoltage due to the offsetting effect connected with the dependence of the electron injection current and the number of recombination centers on surface area of the film. The photocurrent−voltage responses of the dye-sensitized rutile- and anatase films at one-sun light intensity are remarkably close in view of the early stage of rutile material development for solar cells. The photovoltage of the materials is essentially the same, whereas the short-circuit photocurrent of the rutile-based cell is about 30% lower than that of the anatase-based cell. The difference in photocurrent, for the same film thickness, is found to be related to the lesser amount of adsorbed dye, owing to a smaller surface area per unit volume of the rutile film compared with that of the anatase film. Analyses of intensity-modulated photocurrent spectroscopy and scanning electron microscopy data suggest that electron transport is slower in the rutile layer than in the anatase layer due to differences in the extent of interparticle connectivity associated with the particle packing density. Increasing the surface area of the rutile film by producing a more densely packed film of smaller particles is expected to improve the photocurrent. Also, orienting the rutile particles may improve charge transport.

Acknowledgment. This work was supported by the Office of Science, Division of Chemical Sciences (J.v.d.L., and A.J.F.), and the Office of Utility Technologies, Division of Photovoltaics (N.-G. P), U.S. Department of Energy, under contract DE-AC36-99GO10337.

References and Notes

(1) Hagfeldt, A.; Grätzel, M. *Chem. Rev.* **1995**, *95*, 49.
(2) (a) Bedja, I.; Hotchandani, S.; Kamat, P. V. *J. Phys. Chem.* **1994**, *98*, 4133. (b) Ferrere, S.; Zaban, A.; Gregg, B. A. *J. Phys. Chem. B* **1997**, *101*, 4490.
(3) (a) Redmond, G.; Fitzmaurice, D.; Grätzel, M. *Chem. Mater.* **1994**, *6*, 686. (b) Rensmo, H.; Keis, K.; Lindström, H.; Södergren, S.; Solbrand, A.; Hagfeldt, A.; Lindquist, S.-E.; Wang, L. N.; Muhammed, M. *J. Phys. Chem. B* **1997**, *101*, 2598. (c) Rao, T. N.; Bahadur, L. *J. Electrochem. Soc.* **1997**, *144*, 179. (d) Keis, K.; Vayssieres, L.; Lindquist, S.-E.; Hagfeldt, A. *Nanostruct. Mater.* **1999**, *12*, 487.
(4) (a) Sayama, K.; Sugihara, H.; Arakawa, H. *Chem. Mater.* **1998**, *10*, 3825. (b) Guo, P.; Aegerter, M. A. *Thin Solid Films* **1999**, *351*, 290.
(5) Turkovic, A.; Crnjak Orel, Z. *Sol. Energy Mater. Sol. Cells* **1997**, *45*, 275.
(6) El Zayat, M. Y.; Saed, A. O.; El-Dessouki, M. S. *Int. J. Hydrogen Energy* **1998**, *23*, 259.
(7) For example, see: Barbe, C. J.; Arendse, F.; Comte, P.; Jirousek, M.; Lenzmann, F.; Shklover, V.; Grätzel, M. *J. Am. Ceram. Soc.* **1997**, *80*, 3157.
(8) http://www.dupont.com/tipure/coatings/index.html
(9) (a) Wold, A. *Chem. Mater.* **1993**, *5*, 280. (b) Hoffmann, M. R.; Martin, S. T.; Choi, W.; Bahnemann, D. W. *Chem. Rev.* **1995**, *95*, 69.
(10) Park, N.-G.; Schlichthörl, G.; van de Lagemaat, J.; Cheong, H. M.; Mascarenhas, A.; Frank, A. J. *J. Phys. Chem. B* **1999**, *103*, 3308.
(11) Zaban, A.; Ferrere, S.; Sprague, J.; Gregg, B. A. *J. Phys. Chem. B* **1997**, *101*, 55.
(12) Schlichthörl, G.; Park, N.-G.; Frank, A. J. *J. Phys. Chem. B* **1999**, *103*, 782.
(13) Schlichthörl, G.; Huang, S. Y.; Sprague, J.; Frank, A. J. *J. Phys. Chem. B* **1997**, *101*, 8141.
(14) Nazeeruddin, M. K.; Kay, A.; Rodicio, I.; Humphry Backer, R.; Mueller, E.; Liska, P.; Vlachopoulos, N.; Grätzel, M. *J. Am. Chem. Soc.* **1993**, *115*, 6382.
(15) van de Lagemaat, J.; Park, N. G.; Frank, A. J. *J. Phys. Chem. B* **2000**, *104*, 2044.
(16) Cao, F.; Oscam, G.; Meyer, G. J.; Searson, P. C. *J. Phys. Chem.* **1996**, *100*, 17 021.
(17) de Jongh, P. E.; Vanmaekelbergh, D. *Phys. Rev. Lett.* **1996**, *77*, 3427.
(18) Dloczik, L.; Ileperuma, O.; Lauermann, I.; Perer, L. M.; Ponomarev, E. A.; Redmond, G.; Shaw, N. J.; Uhlendorf, I. *J. Phys. Chem. B* **1997**, *101*, 10 281.
(19) de Jongh, P. E.; Vanmaekelbergh, D. *J. Phys. Chem. B* **1997**, *101*, 2716.
(20) Kopidakis, N.; Schiff, E. A.; Park, N.-G.; van de Lagemaat, J.; Frank, A. J. *J. Phys. Chem. B* **2000**, *104*, 3930.
(21) Nelson, J. *Phys. Rev. B* **1999**, *59*, 15374.
(22) Solbrand, A.; Lindström, H.; Rensmo, H.; Hagfeldt, A.; Lindquist, S.-E.; Södergren, S. *J. Phys. Chem. B* **1997**, *101*, 2514.